Cell Cycle 13:2, 303–314; January 15, 2014; © 2014 Landes Bioscience

Chk1 inhibition in p53-deficient cell lines drives rapid chromosome fragmentation followed by caspase-independent cell death

Christopher J Del Nagro[1], Jonathan Choi[1], Yang Xiao[1], Linda Rangell[2], Sankar Mohan[3,†], Ajay Pandita[3,†], Jiping Zha[2,‡], Peter K Jackson[1,§], and Thomas O'Brien[1,*]

[1]Discovery Oncology; Genentech; San Francisco, CA; [2]Department of Pathology; Genentech; San Francisco, CA; [3]Department of Research Diagnostics; Genentech; San Francisco, CA

Current affiliations: [†]OncoMDx; Palo Alto, CA USA; [‡]Crown Bioscience; Jiangsu Province, PR, China; [§]Stanford University Medical Center; Palo Alto, CA USA

Keywords: Chk1, GNE-783, p53, gemcitabine, chemo-potentiation, checkpoint-bypass

Activation of Checkpoint kinase 1 (Chk1) following DNA damage mediates cell cycle arrest to prevent cells with damaged DNA from entering mitosis. Here we provide a high-resolution analysis of cells as they undergo S- and G_2-checkpoint bypass in response to Chk1 inhibition with the selective Chk1 inhibitor GNE-783. Within 4–8 h of Chk1 inhibition following gemcitabine induced DNA damage, cells with both sub-4N and 4N DNA content prematurely enter mitosis. Coincident with premature transition into mitosis, levels of DNA damage dramatically increase and chromosomes condense and attempt to align along the metaphase plate. Despite an attempt to congress at the metaphase plate, chromosomes rapidly fragment and lose connection to the spindle microtubules. Gemcitabine mediated DNA damage promotes the formation of Rad51 foci; however, while Chk1 inhibition does not disrupt Rad51 foci that are formed in response to gemcitabine, these foci are lost as cells progress into mitosis. Premature entry into mitosis requires the Aurora, Cdk1/2 and Plk1 kinases and even though caspase-2 and -3 are activated upon mitotic exit, they are not required for cell death. Interestingly, p53, but not p21, deficiency enables checkpoint bypass and chemo-potentiation. Finally, we uncover a differential role for the Wee-1 checkpoint kinase in response to DNA damage, as Wee-1, but not Chk1, plays a more prominent role in the maintenance of S- and G_2-checkpoints in p53-proficient cells.

Introduction

Genotoxic damage occurring during DNA replication activates the DNA damage response (DDR) pathway, which initiates DNA repair and prohibits mitotic entry until genomic fidelity is restored. There are 2 major DDR pathways that utilize different members of the phosphoinositide 3-kinase-related kinase (PIKKs) family and checkpoint kinases; Ataxia telangiectasia mutated (ATM) that activates Checkpoint kinase 2 (Chk2), and Ataxia telangiectasia and Rad3-related kinase (ATR) that activates the Checkpoint kinase 1 (Chk1).

Inhibition of the DDR pathway with caffeine (ATR/ATM inhibitor) in cells exposed to hydroxyurea (ribonucleotide-reductase inhibitor) results in DNA condensation and "pulverized" chromosomal material when visualized by mitotic spread analysis, a phenomenon termed premature chromosomal condensation (PCC).[1] The overexpression of kinase-defective variants of ATR or Chk1, but not ATM, enabled the PCC phenotype, while the overexpression of wild-type Chk1 specifically blocked PCC in cells lacking functional ATR.[2] Additional characterization utilizing Chk1 and Chk2 siRNA knockdown experiments further supported a role for Chk1 but not Chk2 in preventing premature mitosis in cells exposed to gemcitabine,[3] where the active metabolite (2',2'-Difluoro-2'-deoxycitidine triphosphate) mediates DNA polymerase stalling and induces DNA damage.[4]

Here we use a novel Chk1 kinase selective inhibitor, GNE-783, to probe the kinetics of premature mitotic entry following DNA damage. We show that Chk1 inhibition promotes a very rapid bypass of the mitotic entry checkpoint in cells previously treated with gemcitabine. Premature entry of S-phase-arrested cells with DNA damage into mitosis amplifies the magnitude of the DNA damage with the result that heavily fragmented chromosomes are observed within 4–8 h. Chemopotentiation of gemcitabine-mediated cell death with GNE-783 correlates strongly with the absence of p53 function and the ability to mediate checkpoint bypass. Moreover, cell death and caspase activation only become apparent once cells exit mitosis.

*Correspondence to: Thomas O'Brien; Email: obrien.tom@gene.com
Submitted: 10/04/2013; Accepted: 11/02/2013
http://dx.doi.org/10.4161/cc.27055

Results

GNE-783 enhances DNA damage and potentiates gemcitabine activity

Through a combination of high-throughput screening and structure-guided medicinal chemistry, the ATP competitive-inhibitor, GNE-783 (**Fig. 1A**) was identified.[5,6] This compound is 444-fold selective for inhibition of Chk1 vs. Chk2 (IC_{50} 0.001 μM vs. 0.444 μM).[6] Consistent with previous reports showing that Chk1 inhibitors potentiate activity of DNA damaging agents,[7-12] GNE-783 decreased the EC_{50} of gemcitabine from 0.039 μM to 0.005 μM and increased the maximum percentage of cell death from 25% to 68% (**Fig. 1B**). Moreover, chemo-potentiation was observed at concentrations of GNE-783 that display minimal single agent activity (**Fig. S1**).

Gemcitabine induces DNA damage and activates the ATR DNA damage repair signaling pathway,[13] resulting in phosphorylation of serine 39 of histone H2AX (γH2AX). We measured DNA damage in cells using intracellular flow cytometry and determined both the percentage of cells that stain positive for γH2AX (**Fig. 1C**) and the relative level of DNA damage per cell using the calculated mean fluorescence intensity (MFI) for each cell (**Fig. 1D**). While gemcitabine (0.01 μM) treated cells have detectable but low levels of DNA damage, the concomitant addition of GNE-783 with 0.01 μM gemcitabine increased both the percentage of γH2AX-positive cells and the MFI per cell (**Fig. 1C and D**). At higher concentrations of gemcitabine (0.05 and 0.2 μM), even though most cells are positive for γH2AX (80–90%), there is still a dose-dependent increase in the average intensity of staining per cell with the addition of GNE-783 (**Fig. 1C and D**).

Chk1 inhibition induces S- and G_2-checkpoint bypass

As Chk1 inhibition following DNA damage promotes premature entry into mitosis,[14] we examined DNA content and mitotic index simultaneously by flow cytometry (**Fig. 2A and B**). Exposing HT29 cells to 0.2 μM gemcitabine for 16 h induced a strong S- and G_2-cell cycle arrest (**Fig. 2B**; **Table S1**). After 32 h these cells do not resume cell cycle progression, and by 64 h cell death is apparent (~35% of cells with a sub-2N DNA content) (**Fig. 2B**; **Table S1**). In contrast, the addition of 1 μM GNE-783 to gemcitabine-pretreated cells generated a robust wave of pHH3-positive cells within 4–8 h, and this population included a mix of cells with 4N and <4N DNA content (**Fig. 2B and C**). After 16 h, the majority of cells are pHH3-negative, and there is a corresponding increase in the sub-2N (6% to 32%) and G_1 population of cells (7% to 38%). Similar results were obtained

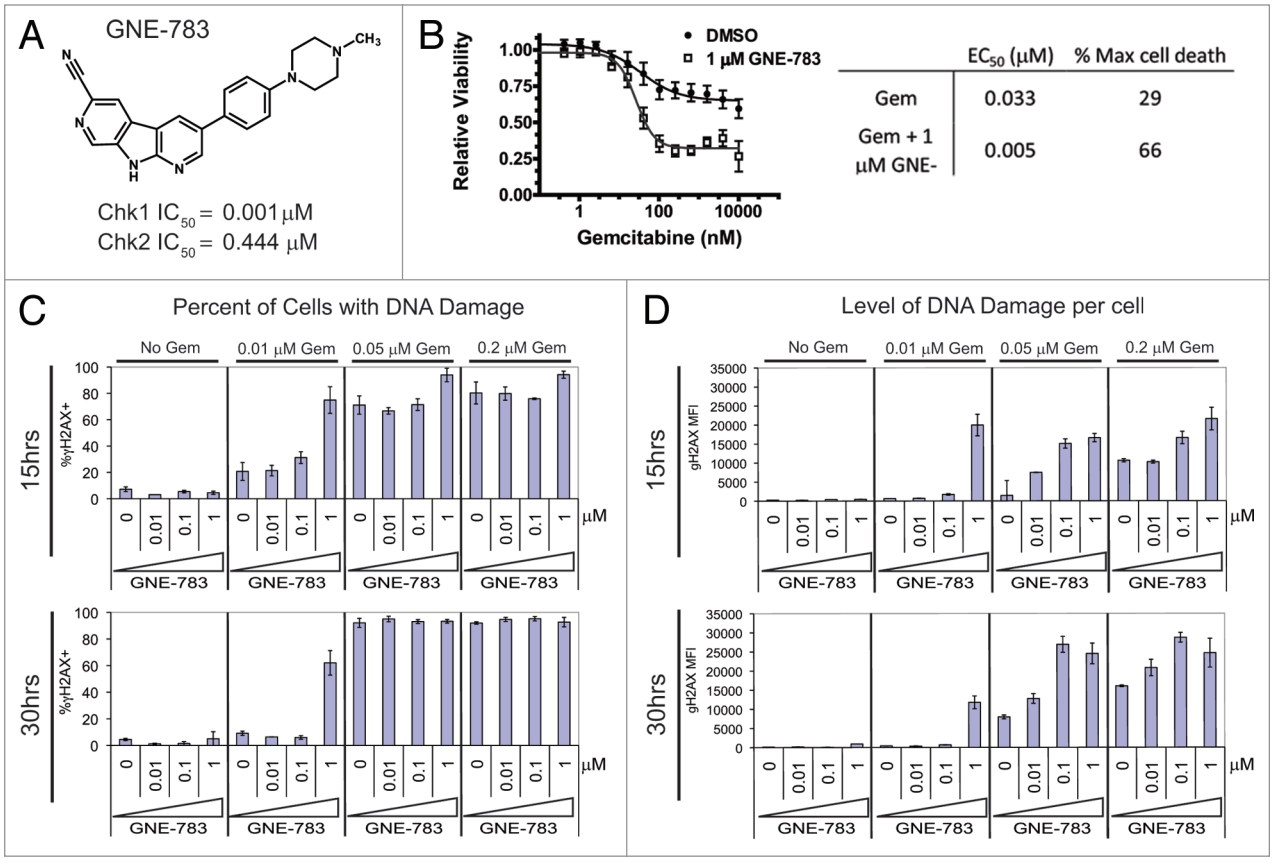

Figure 1. Chk1 inhibition enhances gemcitabine mediated DNA damage. (**A**) Structure of GNE-783 and associated in vitro biochemical IC_{50}s. (**B**) Chemo-potentiation of gemcitabine with 1 μM GNE-783 results in a decrease in cellular viability of HT29 cells in a 72 h proliferation assay. (**C and D**) DNA damage (γH2AX levels) was assessed by intracellular flow cytometry in HT29 cells at 15 and 30 h after the addition of gemcitabine (0.01, 0.05, or 0.2 1 μM) and/or (0.01, 0.1, or 1 μM) GNE-783. The left panel shows the percent of cells staining positive for γH2AX staining (**C**), and the right panel shows the mean fluorescent intensity of γH2AX staining per cell (**D**) (n = 2, ave ± SD shown for both [**C and D**]).

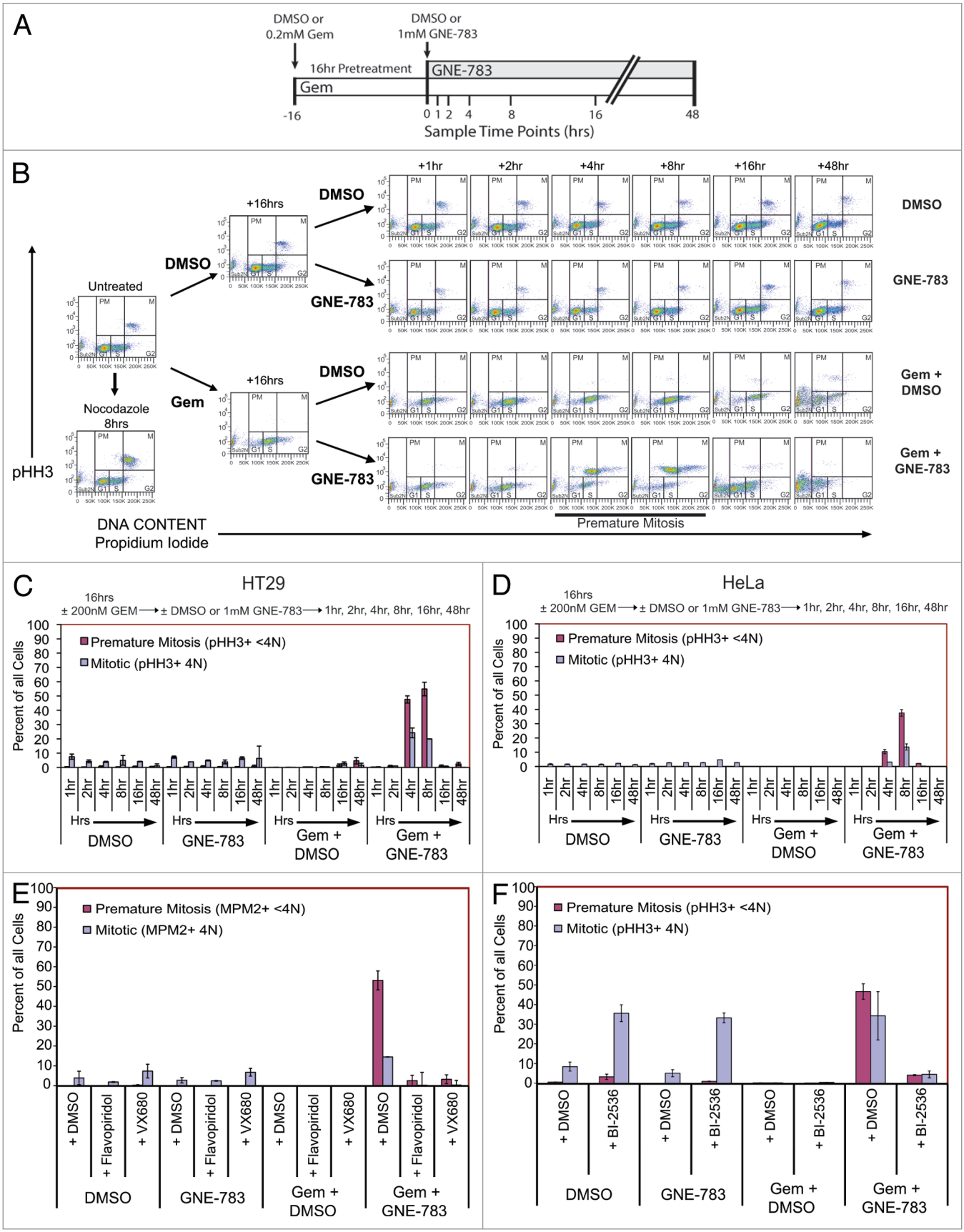

Figure 2. For figure legend, see page 306.

Figure 2 (See previous page). GNE-783 mediates S- and G-checkpoint bypass. (**A**) Schematic illustrating the treatment schedule. (**B**) Cell cycle analysis by intracellular flow cytometry was assessed using propidium iodide for DNA content and phospho-histone H3 for mitotic entry (*y*-axis) in HT29 cells treated as in (**A**). Mitotic cell gating was verified by the addition of 0.1 μM Nocodazole to untreated cells (lower panel). Premature mitosis is indicated at 4 and 8 h post-GNE-783 addition. Quantification of the percent of HT29 (**C**) or HeLa (**D**) cells that are determined to be mitotic ($pHH3^+$ 4N) or premature mitotic ($pHH3^+$ < 4 N). (**E**) HT29 cells were treated as per (**A**), with the addition of 0.3 μM flavopiridol or 1 μM VX-680 concomitant with GNE-783. Both the mitotic ($MPM2^+$ 4N) and the premature mitotic ($MPM2^+$ < 4N) populations were quantified 8 h after GNE-783 addition. (**F**) HT29 cells were treated as in (**A**), with the addition of 0.1 μM BI-2536 concomitant with GNE-783. Both the mitotic and the premature mitotic populations (both by $pHH3^+$) were quantified 8 h after GNE-783 addition and graphed as in (**C**) (n = 2, ave ± SD shown for [**C–F**]).

with HeLa cells (**Fig. 2C**). Thus, inhibition of Chk1 with GNE-783 results in a rapid and coordinated override of the S- and G_2-phase checkpoints.

Inhibition of cdk1/2 (with 0.3 μM Flavopiridol[15]) or Aurora kinases (with 1 μM VX-680[16]) prevented premature mitotic entry as measured by either MPM-2 (**Fig. 2E**) or pHH3 (data not shown) levels; we examined MPM2 status as Aurora kinase B directly phosphorylates serine 10 of histone H3.[17] Plk1 activity is required for mitotic entry after repair of DNA damage,[18,19] but in unperturbed cells, it is required for progression through mitosis.[20] Here we find that while Plk1 inhibition (0.1 μM BI-2536)[20] in gemcitabine-treated cells does not promote entry into mitosis, inhibiting Plk1 and Chk1 in cells pretreated with gemcitabine attenuated the appearance of both the <4N pHH3-positive and 4N pHH3-positive populations (**Fig. 2E**). Thus bypass of both the S- and G_2-checkpoints requires the activity of kinases that normally promote the G_2–M transition.

Inhibition of Chk1 following DNA damage results in dramatic differences in the kinetics of mitotic progression

We utilized live-cell imaging of HeLa cells stably transformed with GFP-tagged histone H2B to track cell cycle progression. In contrast to control cells (**Fig. 3A**, top panel), cells treated with GNE-783 after a 16 h incubation with gemcitabine showed rapid condensation and subsequent fragmentation of nuclear DNA (**Fig. 3A**, bottom panel). In addition, chromosomal materials, which may be lagging chromosomes or fragments of chromosomes, are frequently observed after DNA condensation (**Fig. 3A**).

Single-cell tracking of ~100 individual HeLa cells revealed that unperturbed cells condense their chromosomes asynchronously (**Fig. 3B**; **Video S1**), and 97% of cells underwent at least one mitotic division within 25 h (**Fig. 3C**). The median time to mitotic entry was 11.1 h (**Fig. 3D**) with an average residence time in mitosis of 1.05 ± 0.41 h (**Fig. 3E**), which is similar to previous reports for HeLa cells (~50–60 min).[21] In contrast, 89% of cells treated with gemcitabine remained in S-phase (**Fig. 3B**; **Video S2**).

Inhibition of Chk1 (**Video S3**) modestly accelerated the average time to initial condensation (7.8 vs. 11.1 h in unperturbed cells) (**Fig. 3D**) and slightly prolonged mitotic residence time (1.9 ± 2.0 h vs. unperturbed 1.1 ± 0.81 h) (**Fig. 3E**). These observations are consistent with published data suggesting a role for Chk1 in spindle checkpoint function[22] and chromosome alignment during metaphase.[23,24]

The addition of GNE-783 to gemcitabine-treated cells (**Video S4**) resulted in 76% of cells progressing through mitosis with obvious nuclear fragmentation, while 16% of cells entered but did not exit mitosis (**Fig. 3C**). Chromosome condensation occurred with a median time of 7.1 h (**Fig. 3D**), and the mitotic residence time was markedly longer (5.3 h ± 2.88 h) than in control cells (1.1 ± 0.81 h) (**Fig. 3E**).

Combination treated cells have an abnormal mitotic architecture and display high levels of DNA damage and chromosomal fragmentation

Using electron microscopy, we determined that control cells (**Fig. 4A**, left panel) contained mitotic cells with condensed chromosomes, whereas cells treated with gemcitabine for 24 h (**Fig. 4A**) contained only interphase cells with intact nuclear membranes and diffuse chromosomal material. Cells exposed to gemcitabine for 24 h with 1 μM GNE-783 during the last 8 h (**Fig. 4A**, right panels) had no detectable nuclear membrane, but contained large aggregates of condensed DNA at the cytoplasmic periphery.

Confocal immunofluorescence imaging confirmed that the majority of DNA in combination-treated cells was located outside the metaphase plate (**Fig. 4B**) with a distribution similar to the pattern observed by electron microscopy (**Fig. 4A**). INCENP co-localized with DNA, although some foci aligned along the metaphase plate with small fragments of DNA, suggesting that some centromeres were properly aligning along the metaphase plate. This, along with our live cell imaging (**Fig. 3A**), supports a model of catastrophic failure of the DNA to remain aligned along the metaphase plate.

Exposing cells to gemcitabine induced a gradual increase in γH2AX staining from low ($\gamma H2AX^{Lo}$) to high ($\gamma H2AX^{Hi}$) levels over a period of 64 total hours (16 plus 48 h) (**Fig. 5A**). The addition of 1 μM GNE-783 to cells pretreated with gemcitabine for 16 h rapidly increased $\gamma H2AX^{Hi}$ cells within 4–8 h. These $\gamma H2AX^{Hi}$ cells were pHH3-positive, and their appearance correlates with the timing of mitotic entry (**Fig. 3D**) and the re-localization of DNA observed by electron microscopy and immunofluorescence imaging (**Fig. 4A and B**). Utilizing an Amnis ImageStream flow microscope we determined that the $\gamma H2AX^{Hi}$ staining in pHH3-positive cells was due to increased staining per foci and not to an increase in foci size or number (**Fig. S2**).

To investigate the impact of high levels of DNA damage on chromosome structure, we performed spectral karyotyping (SKY) of chromosomes in HT29 cells.[25] Coincident with S- and G_2-checkpoint bypass, we note 2 forms of chromosomal fragmentation by SKY imaging; cells exhibiting type 1 fragmentation contain larger and more identifiable chromosomal fragments that are condensed but characteristically more diffuse than normal mitotic chromosomes, while type 2 fragmentation contains extremely high levels of fragmentation of all chromosomes (**Fig. 5B and C**). As fewer cells with type

1 fragmentation were observed at 8 h compared with 4 h, we suspect that type 1 fragmentation may represent a transition state toward type 2 fragmentation.

The recombinase Rad51 binds to single-stranded DNA at sites of damage and displaces replication protein A (RPA) to promote homologous DNA repair.[26] Rad51 foci were found in HT29 cells exposed to 0.2 μM gemcitabine for 16 h (**Fig. 5D**), indicating that cells were promoting homologous recombination in response to gemcitabine-mediated DNA damage. The addition of 1 μM GNE-783 for 8 h following gemcitabine resulted in the formation of pHH3-positive cells, all of which were Rad51-negative. Interestingly, cells that were pHH3-negative still contained Rad51 foci, suggesting that in combination-treated cells Rad51 foci can still form, but these foci are lost as cells progress into mitosis.

Cell death in combination treated cells is driven by multiple modes of death

A fluorescently labeled antibody directed against active caspase-3 was used to probe levels of caspase-3 in individual cells. Appearance of active caspase-3 only occurred only after cells had exited mitosis, as high levels of active caspase-3 were exclusively detected in pHH3-negative cells (**Fig. 6A**) (these cells were verified to be $\gamma H2AX^{Hi}$ [data not shown]). Thus, cells containing active caspase-3 and pHH3 are mutually exclusive.

We also examined activation of caspase-2 using a caspase-2 luminescence substrate (**Fig. 6B**) and by western blot analysis

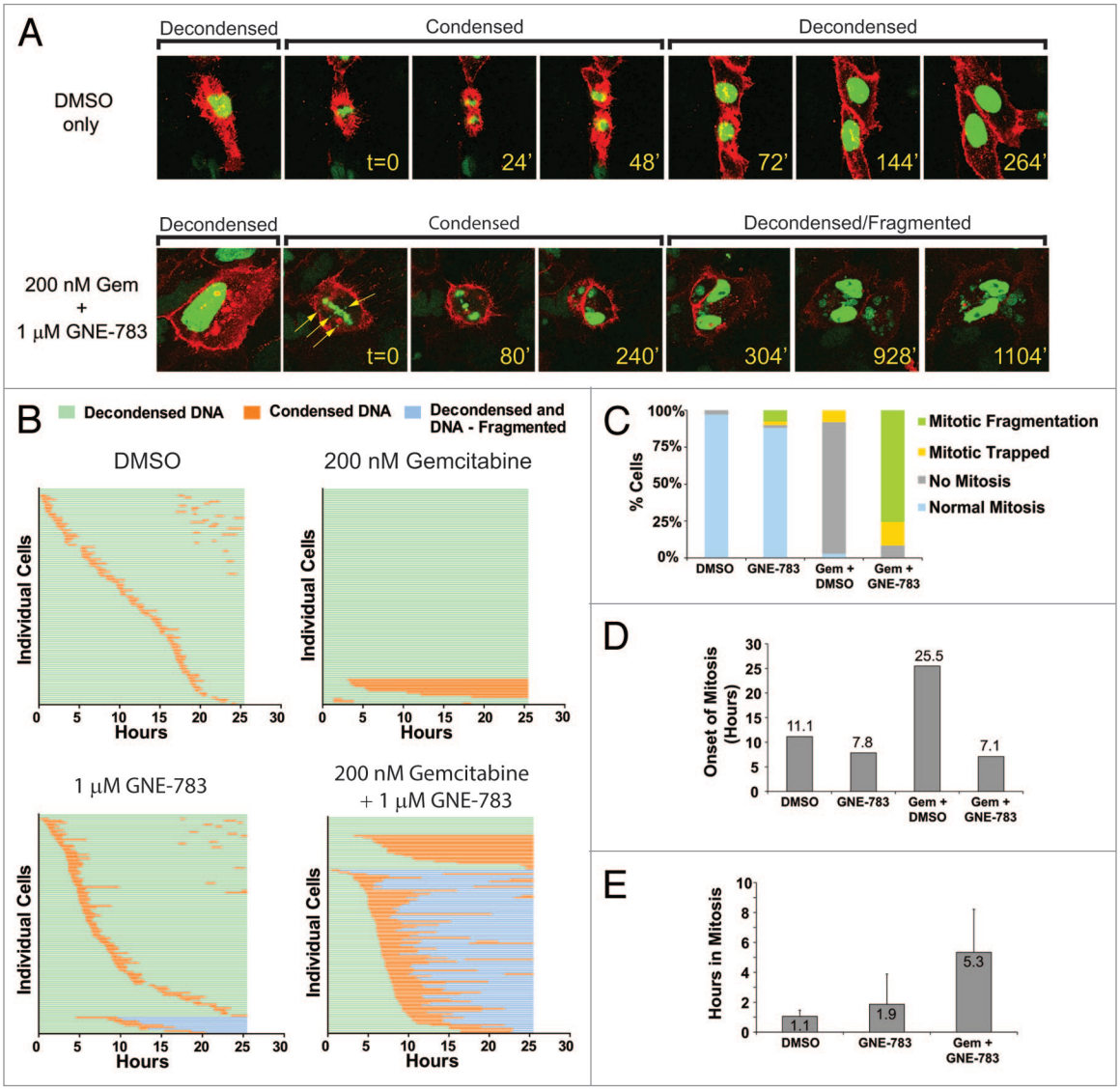

Figure 3. Chk1/gemcitabine combination promotes rapid chromosome fragmentation. (**A**) Live cell imaging of HeLa cells expressing GFP tagged Histone H2B (GFP-H2B) and treated with CellLight™ Plasma Membrane-RFP (PM-RFP). Representative images are from control cells or cells treated with gemcitabine for 16 h and 1 μM GNE-783 for various times (as in **Fig. 2A**). Nuclear condensation is marked as time 0 (t = 0). Arrows indicate chromosomal material that fails to congress to the metaphase plate. (**B**) Single cell tracking by live cell imaging of ~100 individual HeLa cells treated as shown in **Figure 2A**. Image acquisition was initiated after gemcitabine treatment but prior to GNE-783 addition and images were taken every 8 min for 25 h. (**C**) Individual outcomes of ~100 single cells following each treatment. (**D**) Median time to onset of mitosis following the addition of DMSO or GNE-783. (**E**) Mean duration of mitosis with standard deviations for the indicated treatments.

of lysates from the same experiment to probe for the active p19 subunit of caspase-2 (**Fig. 6B**). While treatment of HT29 cells with or without 0.2 μM gemcitabine for 48 h did not result in a change in caspase-2 activity or the generation of the cleaved mature subunit, the addition of 1 μM GNE-783 for the last 12 or 24 h of gemcitabine treatment resulted in an increase in caspase-2 luminescence and an increase in the presence of the mature p19 large subunit.

Exposure of cells to gemcitabine alone for 48 h generated an increase in the percentage of caspase-3-positive cells, and the pan-caspase inhibitor z-VAD-FMK reduced the percentage of caspase-3-positive cells and the percentage of cells with a sub-2N DNA content (**Fig. 6C**). Cells treated with gemcitabine for 16 h and then 1 μM GNE-783 for an additional 32 h also generated caspase-3 positive cells, and the percentage of these cells could be reduced with z-VAD-FMK. However, inhibition of caspase-3 only had a modest impact on the percentage of cells with a sub-2N DNA content, suggesting minimal effect on overall levels of cell death.

Finally, we used electron microscopy to examine cell morphology 20 h after the addition of 1 μM GNE-783 to cells pretreated with 0.2 μM gemcitabine for 16 h. While quantitation of each phenotype was not possible due to low numbers of cells in these visual fields, we noted a mixture of apoptotic (rounded cells, membrane blebbing) and necrotic (translucent cytoplasm, large vacuolated mitochondria) features in cells that fail to reform nuclear membranes (**Fig. 6D**). A third cellular fate was multi-nucleation, and these were the only cells found to reform their nuclear membranes (**Fig. 6D**, right panel).

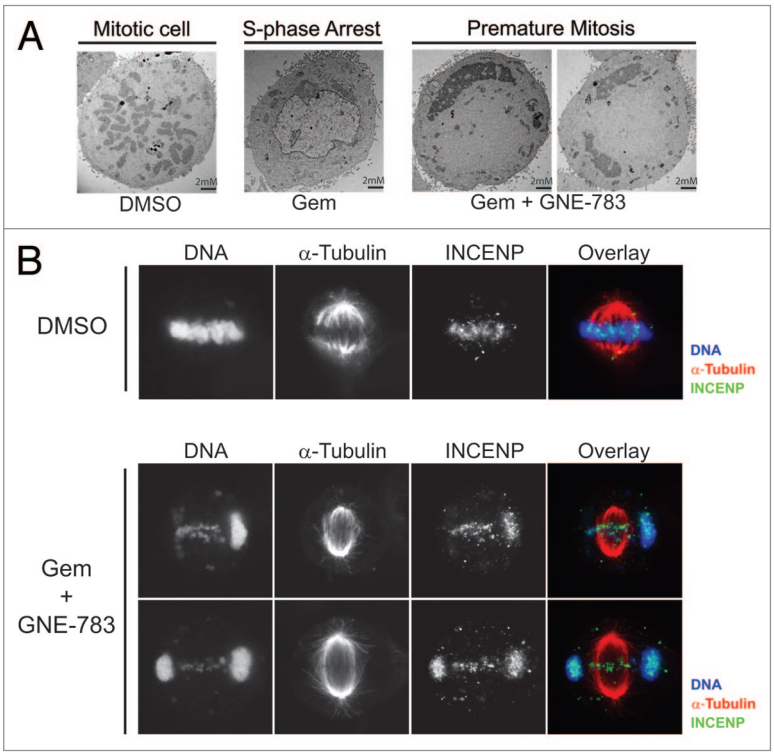

Figure 4. Dramatic morphological changes associated with premature mitosis are observed in GNE-783/gemcitabine treated cells. (**A**) Transmission electron microscope imaging of HT29 cells treated with either DMSO for 24 h, with gemcitabine for 24 h, or pretreated with 0.2 μM gemcitabine for 16 h and then 1 μM GNE-783 for 8 h (right 2 images). (**B**) Mitotic cells imaged by immunofluorescene staining of DNA with Hoescht (blue), spindles with anti-tubulin (red) and kinetechores with anti-INCENP (green) in HT29 cells treated as in (**A**).

p53 status, but not p21 status, correlates with premature mitotic entry

The p53-deficient cell lines HeLa, HT29, and MiaPaCa-2 showed high levels of potentiation of gemcitabine activity by GNE-783, whereas the p53 wild-type cell lines HCT116 and A549 cells showed minimal levels of potentiation (**Fig. 7A**). This is consistent with previous data implicating a role for p53 in chemopotentiation following Chk1 inhibition.[6,12,27-29] Utilizing isogenic HCT116 cells that are either wild-type or deficient for p53 or for p21 (the latter being a p53 transcriptional target and checkpoint regulator[30,31]), we found that p53, but not p21, deficiency enables potentiation (**Fig. 7B**).

Similar to potentiation of cell death, checkpoint bypass occurred in p53-deficient cell lines (HeLa, HT29, and MiaPaca-2), but not in p53 wild-type cell lines (HCT116 and A549) (**Fig. 7C**); moreover, checkpoint bypass also correlated with p53, but not p21 status (**Fig. 7D**). We also examined other time points (2, 4, 16, and 48 h) and verified that checkpoint bypass was not simply delayed in p21-deficient cells (data not shown). Thus, there is a correlation between high levels of potentiation and the ability of cells to rapidly bypass the S- and G_2-checkpoints (**Fig. 7E**).

Mitotic entry is dependent on the activity of the cyclin B/cdk1 complex, which is inhibited by Wee-1 kinase phosphorylation of tyrosine 15 on cdk1.[32] Mitotic entry coincides with removal of this inhibitory phosphorylation by the Cdc25C phosphatase.[33] Following DNA damage, Chk1 phosphorylates Cdc25C to promote its degradation, and thus the Cyclin B/cdk1 complex remains phosphorylated and thus inactive.[33] Two different wee-1 kinase inhibitors (Wee1-I and MK1776) promoted premature mitotic entry in both wild-type and p53-deficient HCT116 cells that were previously treated with gemcitabine for 16 h (**Fig. 7F**), with the response in p53-deficient cells being greater than that in p53 wild-type cells. In contrast, premature mitotic entry in response to Chk1 inhibition only occurred in p53-deficient cells. Thus, in p53-proficient cells, Wee-1 has a role in maintaining cell cycle arrest following DNA damage, indicating a distinct functional difference from Chk1.

Discussion

Chk1 has roles both in replication initiation[34,35] and in maintaining high replication rates in unperturbed cells.[35,36] Additionally, Chk1 is required to maintain the S- and G_2-cell cycle checkpoints to prevent cell cycle progression in the presence of DNA damage,[7,11,37,38] and thus is considered to be an important therapeutic target.[39] There are only a few examples showing bypass of both the S- and G_2-checkpoints in response to Chk1

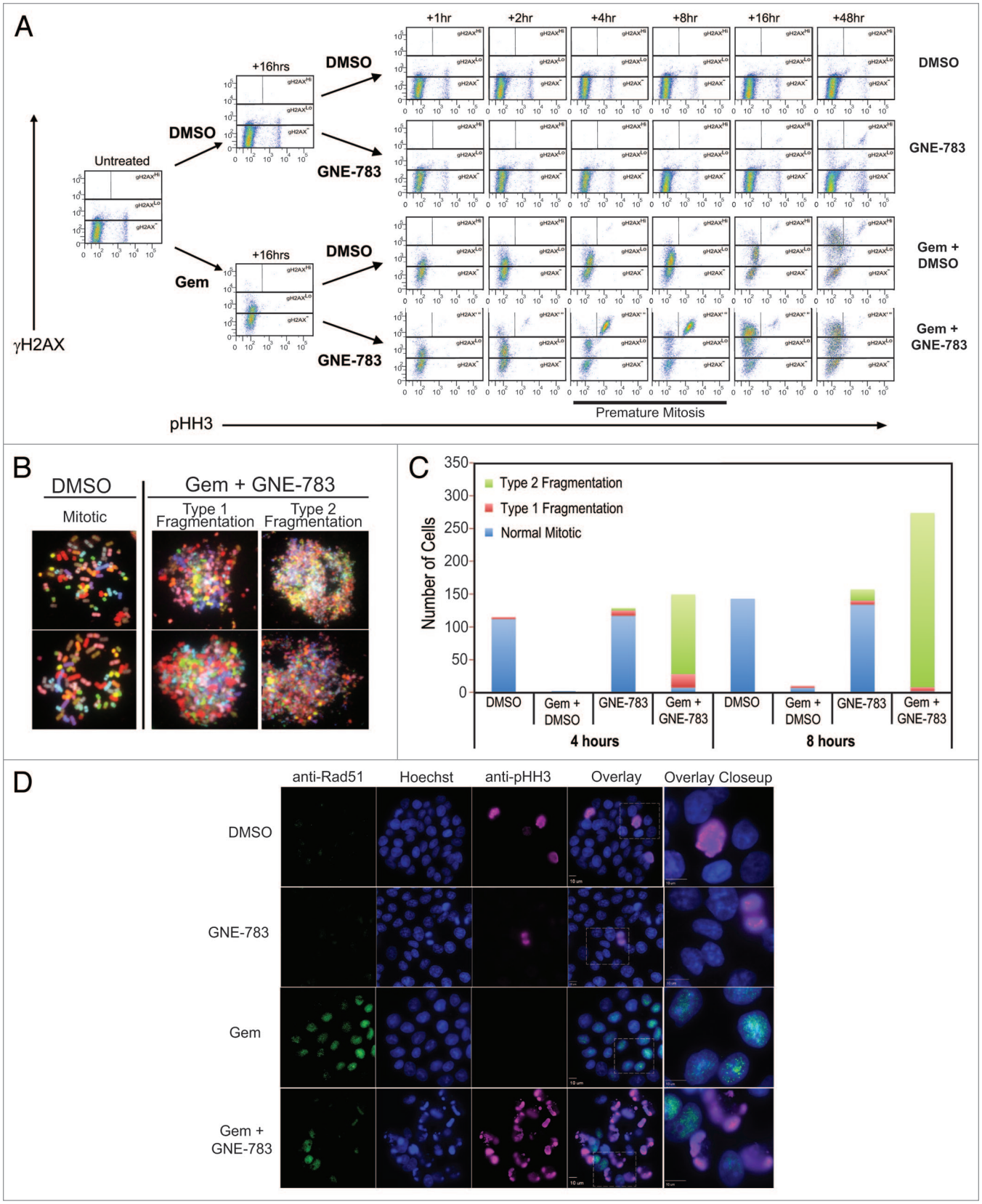

Figure 5. For figure legend, see page 310.

Figure 5 (See previous page). Premature mitosis coincides with increased DNA damage and fragmentation. (**A**) DNA damage analysis by intracellular flow cytometry using anti-γH2AX for DNA damage and phospho-histone H3 (ser10) in HT29 cells treated as in **Figure 2A**. Premature mitotic (<4N DNA) and mitotic cells (4N DNA) pHH3^{+} cells are indicated at 4 and 8 h post-GNE-783 addition and contain high γH2AX (γH2AX^{Hi}) staining compared with gemcitabine only treated cells. (**B**) Spectral karyotyping (SKY) imaging of HT29 cells treated with DMSO (24 h) or with 0.2 μM gemcitabine for 16 h followed by the addition of 1 μM GNE-783 for 8 h. (**C**) Quantitation of normal mitosis, Type I and II fragmentation, observed in part (**B**) displayed as number of observed cells. (**D**) Immunofluorescene imaging of Rad51 foci with anti-Rad51 (green), DNA with Hoescht (blue), and anti-phospho-histone H3 (ser10) (purple) in HT29 cells treated as in part (**A**), with GNE-783 only present for 8 h.

inhibition;[40-42] moreover, the fate of cells was examined only at a low resolution, leaving an incomplete understanding of the events that occur between inhibition of Chk1 and cell death. Here we provide a high-resolution analysis of the fate of cells as they undergo S- and G_2-checkpoint bypass, and provide mechanistic insight into the events leading to chromosome fragmentation and cell death.

Our analysis reveals that bypass of the S- and G_2-cell cycle checkpoints occurs rapidly following Chk1 inhibition and requires both the cdk1/2 and Aurora mitotic kinases. Moreover,

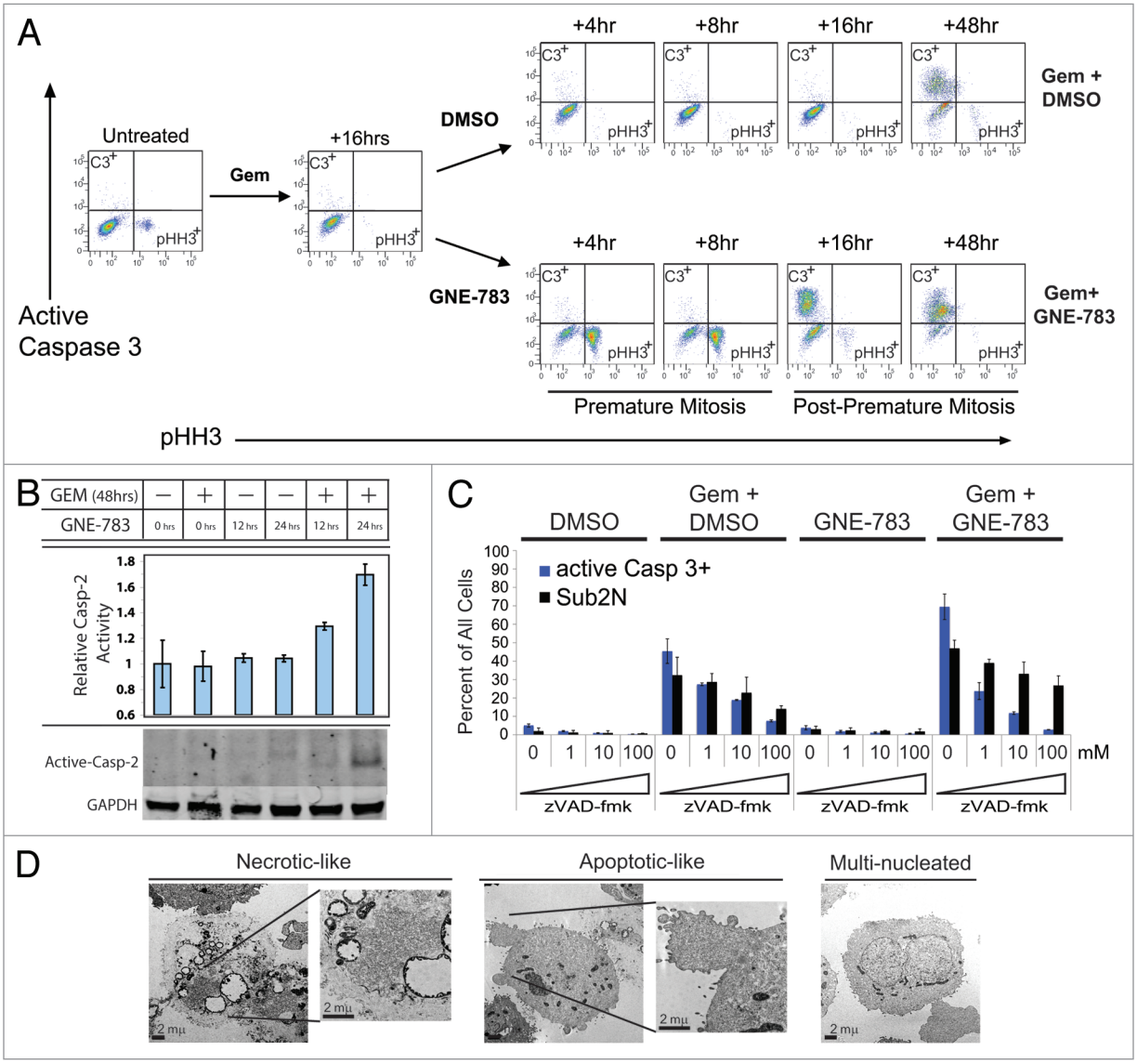

Figure 6. Caspase activation in combination-treated cells only occurs after HT29 cells exit mitosis. (**A**) Caspase-3 activation by intracellular flow cytometry was detected using anti-active-caspase 3 and phospho-histone H3 (ser10) antidbodies in HT29 cells treated as in **Figure 2A**. (**B**) Caspase-2 activity was determine by a Caspase-Glo 2 assay after 48 h of 0.2 μM gemcitabine treatment or with the addition of 1 μM GNE-783 for the final 12 or 24 h (n = 2, ave ± SD shown). The cleaved form of the large subunit of caspase-2 (p19) was assessed in the same samples by western blot analysis (image cropped; full-length blot is presented in **Fig. S3**). (**C**) A dose curve of the pan-caspase inhibitor zVAD-fmk (0, 1, 10, and 100 μM) and its effects on active caspase-3 and cell death (Sub2N) in cells treated with 0.2 μM gemcitabine for 16 h and then DMSO or GNE-783 for 32 h (n = 3, ave ± SD shown). (**C**) Enlectron microscopic imaging of cells after treatment with 0.2 μM gemcitabine for 16 h and then 1 μM GNE-783 for 20 h.

inhibition of Plk1 following DNA damage and Chk1 inhibition prevents checkpoint bypass, indicating that Plk1 is required for entry into mitosis, consistent with a proposed role for Chk1 in negatively regulating Plk1 following DNA damage.[24]

It was previously noted that cells exposed to gemcitabine and the Chk1 inhibitor PD-321852 simultaneously had an attenuated ability to form Rad51 foci.[43] Here we extend this analysis, and show that Rad51 foci that are formed in response to gemcitabine can still be detected after Chk1 inhibition. However, Rad51 foci are only lost in cells that have progressed into mitosis. While it's possible that Chk1 inhibition following DNA damage reduces or prevents the formation of Rad51 foci (either by destabilizing existing Rad51 foci or by preventing the reformation of foci), cells that have progressed into mitosis have clearly lost these foci.

The observation that chromosome fragmentation occurs during mitotic catastrophe has been noted in previous studies. In particular, an early study implicated the ATR–Chk1 pathway as an important regulator of fragmentation.[2] Premature entry into mitosis also results in the failure to correctly align chromosomes along the metaphase plate (**Figs. 3A and 4B**).

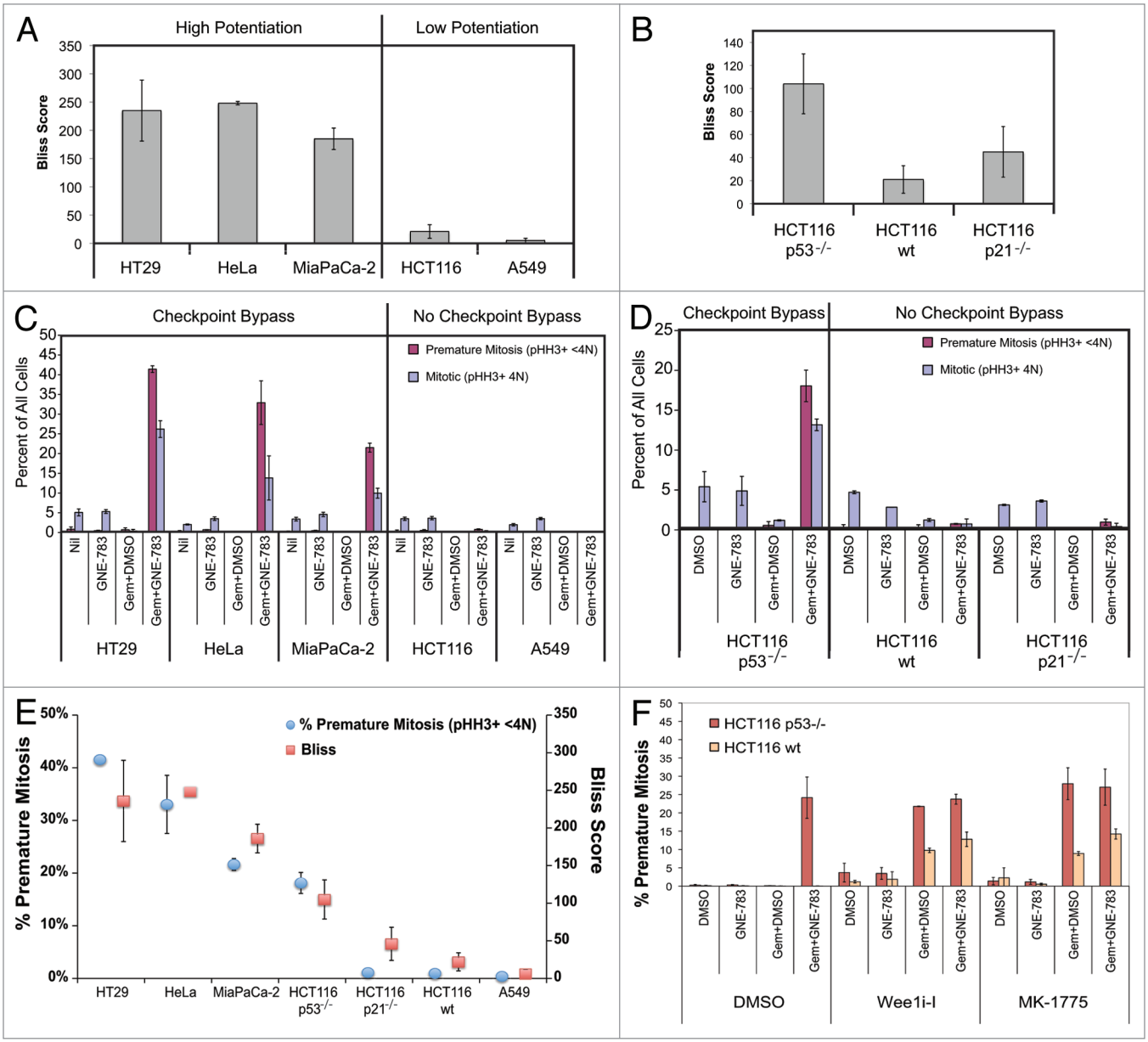

Figure 7. GNE-783/gemcitabine mediated S- and G_2-checkpoint bypass in HT29 cells correlates with chemo-potentiation and p53 status. (**A**) Chemo-potentiation of GNE-783/gemcitabine activity after 72 h in the indicated cell lines. (**B**) Comparison of chemo-potentiation of gemcitabine activity with GNE-783 in isogenically matched HCT116 cells (n = 2, ave ± SD shown for both [**A and B**]). (**C**) The indicated cell lines were exposed to 0.2 μM gemcitabine for 16 h and then 1 μM GNE-783 for 8 h and cell cycle distribution determined as described in **Figure 2C**. (**D**) Genetically matched HCT116 cells were treated and assayed as described in (**C**). (**E**) Correlation between Bliss score and bypass of the S- and G_2-checkpoints across cell lines. (**F**) Cells were exposed to DMSO or 0.2 μM gemcitabine for 16 h, and then DMSO, 1 μM GNE-873, 3 μM Wee1-I, or 1 μM MK1776 for an additional 8 h. Cell cycle analysis was performed as described in **Figure 2C**. (n = 2, ave ± SD shown for [**C–F**]).

However, some chromosomes (or chromosomal fragments) are frequently observed to lag behind and never correctly align along metaphase plate. The timing of DNA redistribution through the cell corresponds with the timing of high levels of chromosomal fragmentation that is observed by SKY imaging (**Fig. 5B and C**), suggesting that fragmentation and redistribution are coincident. Given the role of Rad51 in homologous recombination,[44] the collapse of Rad51 foci may attenuate homologous recombination, resulting in enhanced DNA damage as cells enter mitosis. This is consistent with our observation that the intensity of γH2AX foci staining differentiates $\gamma H2AX^{Lo}$ from $\gamma H2AX^{Hi}$ cells as they enter mitosis (**Fig. S2**). While it remains unclear what drives fragmentation, it is likely a combination of both the presence of double-strand breaks in DNA along with the mechanical sheer forces that chromosomes are exposed to as they condense and align along the metaphase plate. Finally, unlike a previous report that observed tetraploidization of established cell lines that are haploinsufficient for Chk1 (DLD1 and HCT116 cells), we have not observed any evidence of endoreduplication in studies that have examined DNA content at 48 h following Chk1 inhibition.

Inhibition of Chk1 following DNA damage leads to checkpoint bypass followed by mitotic catastrophe;[41,45,46] however, the exact nature or timing of the events leading to cell death has been poorly defined. The presence of highly fragmented DNA in mitotic cells is insufficient to lead to caspase activation (**Fig. 6A**) and is consistent with a model whereby caspase activation is prevented during mitosis.[47] Additionally, z-VAD-FMK (**Fig. 6C**) or a caspase-2 specific inhibitor (data not shown) only modestly reduced the percentage of cells with a sub-2N DNA content. These results, along with our EM analysis, support a minimal role for apoptosis in cell death driven by premature chromosome condensation.

While p53 status can impact the level of chemopotentiation when cells are exposed to gemcitabine and Chk1 inhibitors,[12,28,48] it was not clear what contribution p53 plays in maintaining either the S- or the G_2-checkpoints, nor how p53 status may impact premature chromosome condensation. We show that inhibition of Chk1 following gemcitabine treatment in p53-deficient cells, but not p21-deficient cells, induces bypass of the S- and G_2-checkpoints (**Fig. 7D**) and supports high levels of chemopotentiation (**Fig. 7B**). Recently, it was shown that p21 deficiency in vivo sensitized normal murine cells to a combination of irinotecan and UNC-01,[49] a non-selective Chk1 inhibitor. It is not clear why these results are in contrast to ours, although we note that not only did this study use a different chemotherapeutic, but it also used a less selective Chk1 inhibitor. Nevertheless, our data indicates that downstream targets of p53 other than p21 are important for maintaining the S- and G_2-checkpoints following DNA damage. One potential p53 target that may be important for preventing checkpoint bypass is Cyclin B1. In this case, p53 can directly bind to and repress transcription of the Cyclin B1 gene;[50] thus, cells lacking p53 activity may therefore be more poised to enter mitosis following Chk1 inhibition due to elevated Cyclin levels. In support of this, it was previously noted that high Cyclin B1 levels correlated with enhanced sensitivity to a Chk1 inhibitor.[51] It is also possible that other p53 target(s) may be responsible for modulating the ability of a cell to maintain a G_2-arrest in response to DNA damage.

Even though the function of wee-1 in checkpoint control[52] is similar to Chk1, both kinases function in parallel pathways whose eventual target is to modulate cdc2 (cdk1) activity. Unlike inhibition of Chk1, which results in checkpoint bypass strictly in p53-deficient HCT116 cells, inhibition of wee-1 can induce checkpoint bypass in p53 wild-type cells, although the level of bypass observed is less than that observed in p53-deficient cells (**Fig. 7F**). Thus, our data reveals that Chk1 and Wee-1 are not equivalent kinases with respect to checkpoint maintenance and stringency of p53 status.

The anti-metabolite gemcitabine (2',2'-Difluoro-2'-deoxycitidine) is the standard of care for a number of indications including first line advanced or metastatic adeno-pancreatic cancer. As response rates are typically low (5-y survival rate of 15–25%[53]), novel agents that synergize the activity of gemcitabine and enhance survival response rates are desired. Here we show that inhibition of Chk1 with GNE-783 following DNA damage induced with gemcitabine rapidly drives p53-defective cells into mitosis and enhances DNA damage, chromosome fragmentation, and cell death. Thus, small-molecule Chk1 inhibitors such as GNE-783 are potential candidates that may help increase the clinical response rate of gemcitabine.

Materials and Methods

Chemicals and reagents

Gemcitabine (Eli-Lilly), flavopiridol (F3055; Sigma-Aldrich), VX680 (T2304; LC Labs), wee1i-I (681640; EMD-Millipore), BI-2536 and MK-1776 (S1109 and S1525; Selleck Chemicals), zDEVD-fmk (550378; BD PharMingen), and MG132 (C2211; Sigma-Aldrich) were resuspended in DMSO at 10 mM stock concentration. zVAD-FMK (G7231; Promega) was purchased as a 20 mM stock solution.

Cell lines

HT29, HCT116, HeLa, A549, and MiaPaCa-2 cells were obtained from our in-house tissue culture cell bank (original source was ATCC). Isogenic HCT116 $p53^{-/-}$ and wild-type counterparts were obtained from Horizon, while isogenic $HCT116p21^{-/-}$ and wild-type counterparts were obtained from the Bert Vogelstein Lab.

Cell viability, caspase assays

Cell viability was assessed using Cell-titer Glo (G7570; Promega) readout after 72 h. Caspase-2 luminescence assays were performed using Caspase-Glo 2 Assay (G0940; Promega) in the presence of the proteosomal inhibitor MG132 (60 μM) and the Caspase-3 specific inhibitor z-DEVD-fmk at 60 μM.

Bliss analysis

Bliss analysis compares the observed reduction in viability to the expected reduction in viability if 2 independent agents are additive.[54] A bliss score of >0 indicates synergistic activity, and the higher the bliss score the greater the synergy.

Western analysis

Proteins were detected using anti-Caspase 2 (MAB3507; Millipore) and anti-GAPDH (D16H11; Cell Signaling

Technologies) antibodies. After incubation with secondary anti-rat and anti-rabbit secondary antibodies (926-32219 and 926-68071; Li-Cor) membranes were imaged using an Odyssey IR Fluorescence Imaging System.

Intracellular multi-parameter flow cytometry

Intracellular flow was performed with anti-phospho-histone H3-AF488 (3465; Cell Signaling Technologies), anti-phospho-histone H2AX-AF647 (9720; Cell Signaling Technologies), anti-active-Caspase 3-V450 (560627; BD Horizon), and propidium iodide (P4864; Sigma). Data was collected using a LSRII flow cytometer (BD Biosciences) and analyzed with FlowJo (TreeStar Inc).

Live cell imaging

HeLa cells were transfected with H2B-GFP and Cell-Light Plasma Membrane-RFP using BacMam technology (C10128 and C10608 respectively; Invitrogen). Images were taken every 8 min on a Nikon A1-R Confocal Microscope for a total of 25 h and compiled using the NIS-Elements Imaging software.

EM analysis

Cells were fixed in 1/2 Karnovsky fixative, washed, and post-fixed in 1% osmium textroxide. Samples were dehydrated by ethanol washes followed by a propylene oxide wash and Eponate 12 embedding (18005; Ted Pella Inc). Semi-thin sections (300 μm) cut by Leica Ultracut UCT were stained with toluidine blue for light level (LM) examination. Thin sections (80 μm) stained with uranyl acetate and lead citrate were examined by TEM (JEOL JEM-1400).

Spectral karyotyping (SKY)

Cells were processed as described.[25] The SKY KIT from Applied Spectral Imaging (Applied Spectral Imaging) was used for Spectral Karyotyping with processing according to the manufacturer's instructions.[55,56] Spectral images were acquired and analyzed with a HiSKY Imaging System attached to an Olympus B61 microscope. After acquiring ~100 frames of the same image differing from each other only by optical path difference, images were analyzed using the HiSKY software. For every chromosomal region, identity was determined by spectral emission; pseudo-color classifications aided in the delineation of specific aberrations.

Immunofluorescence imaging

Cells plated on 96-well glass bottom plates (25892; E&K Scientific) were stained with Hoechst 33342 (H3570; Molecular Probes), mouse anti-α-tubulin (DM1A; Santa Cruz Biotechnology), rabbit anti-INCENP (ab36453; abcam), rabbit anti-phospho-histone H3-AF647 (3458BC; Cell Signaling Technologies), mouse anti-Rad51 (NB100–148; Novus Biologicals), and anti-mouse-IgG-AF647 (A31571; Invitrogen), or anti-rabbit-IgG-AF488 (A21206; Invitrogen). Confocal imaging was performed using a SP5 Confocal microscope (Leica).

Disclosure of Potential Conflicts of Interest

No potential conflicts of interest were disclosed.

Acknowledgments

The authors would like to thank the Genentech gCell group (Richard Neve, Suresh Selvaraj, and Mamie Yu) for cell line maintenance.

Supplemental Materials

Supplemental materials may be found here:
www.landesbioscience.com/journals/cc/article/27055

References

1. Schlegel R, Pardee AB. Caffeine-induced uncoupling of mitosis from the completion of DNA replication in mammalian cells. Science 1986; 232:1264-6; PMID:2422760; http://dx.doi.org/10.1126/science.2422760
2. Nghiem P, Park PK, Kim Y, Vaziri C, Schreiber SL. ATR inhibition selectively sensitizes G1 checkpoint-deficient cells to lethal premature chromatin condensation. Proc Natl Acad Sci U S A 2001; 98:9092-7; PMID:11481475; http://dx.doi.org/10.1073/pnas.161281798
3. Morgan MA, Parsels LA, Parsels JD, Mesiwala AK, Maybaum J, Lawrence TS. Role of checkpoint kinase 1 in preventing premature mitosis in response to gemcitabine. Cancer Res 2005; 65:6835-42; PMID:16061666; http://dx.doi.org/10.1158/0008-5472.CAN-04-2246
4. Mini E, Nobili S, Caciagli B, Landini I, Mazzei T. Cellular pharmacology of gemcitabine. 2006:v7-12
5. Dyke JH, Ellwood C, Gancia E, Gazzard LJ, Goodacre S, Kintz S, Lyssikatos J, Macleod C, Williams K. Diazacarbazoles and methods of use. World Intellectual Property Organization: Genentech Inc. 2009
6. Xiao Y, Ramiscal J, Kowanetz K, Del Nagro C, Malek S, Evangelista M, Blackwood E, Jackson PK, O'Brien T. Identification of preferred chemotherapeutics for combining with a CHK1 inhibitor. Mol Cancer Ther 2013; 12:2285-95; PMID:24038068; http://dx.doi.org/10.1158/1535-7163.MCT-13-0404
7. Blasina A, Hallin J, Chen E, Arango ME, Kraynov E, Register J, Grant S, Ninkovic S, Chen P, Nichols T, et al. Breaching the DNA damage checkpoint via PF-00477736, a novel small-molecule inhibitor of checkpoint kinase 1. Mol Cancer Ther 2008; 7:2394-404; PMID:18723486; http://dx.doi.org/10.1158/1535-7163.MCT-07-2391
8. Guzi TJ, Paruch K, Dwyer MP, Labroli M, Shanahan F, Davis N, Taricani L, Wiswell D, Seghezzi W, Penaflor E, et al. Targeting the replication checkpoint using SCH 900776, a potent and functionally selective CHK1 inhibitor identified via high content screening. Mol Cancer Ther 2011; 10:591-602; PMID:21321066; http://dx.doi.org/10.1158/1535-7163.MCT-10-0928
9. Montano R, Chung I, Garner KM, Parry D, Eastman A. Preclinical development of the novel Chk1 inhibitor SCH900776 in combination with DNA-damaging agents and antimetabolites. Mol Cancer Ther 2012; 11:427-38; PMID:22203733; http://dx.doi.org/10.1158/1535-7163.MCT-11-0406
10. Morgan MA, Parsels LA, Zhao L, Parsels JD, Davis MA, Hassan MC, Arumugarajah S, Hylander-Gans L, Morosini D, Simeone DM, et al. Mechanism of radiosensitization by the Chk1/2 inhibitor AZD7762 involves abrogation of the G2 checkpoint and inhibition of homologous recombinational DNA repair. Cancer Res 2010; 70:4972-81; PMID:20501833; http://dx.doi.org/10.1158/0008-5472.CAN-09-3573
11. Tse AN, Rendahl KG, Sheikh T, Cheema H, Aardalen K, Embry M, Ma S, Moler EJ, Ni ZJ, Lopes de Menezes DE, et al. CHIR-124, a novel potent inhibitor of Chk1, potentiates the cytotoxicity of topoisomerase I poisons in vitro and in vivo. Clin Cancer Res 2007; 13:591-602; PMID:17255282; http://dx.doi.org/10.1158/1078-0432.CCR-06-1424
12. Zabludoff SD, Deng C, Grondine MR, Sheehy AM, Ashwell S, Caleb BL, Green S, Haye HR, Horn CL, Janetka JW, et al. AZD7762, a novel checkpoint kinase inhibitor, drives checkpoint abrogation and potentiates DNA-targeted therapies. Mol Cancer Ther 2008; 7:2955-66; PMID:18790776; http://dx.doi.org/10.1158/1535-7163.MCT-08-0492
13. Ewald B, Sampath D, Plunkett W. H2AX phosphorylation marks gemcitabine-induced stalled replication forks and their collapse upon S-phase checkpoint abrogation. Mol Cancer Ther 2007; 6:1239-48; PMID:17406032; http://dx.doi.org/10.1158/1535-7163.MCT-06-0633
14. Ma CX, Janetka JW, Piwnica-Worms H. Death by releasing the breaks: CHK1 inhibitors as cancer therapeutics. Trends Mol Med 2011; 17:88-96; PMID:21087899; http://dx.doi.org/10.1016/j.molmed.2010.10.009
15. Shapiro GI. Cyclin-dependent kinase pathways as targets for cancer treatment. J Clin Oncol 2006; 24:1770-83; PMID:16603719; http://dx.doi.org/10.1200/JCO.2005.03.7689

16. Harrington EA, Bebbington D, Moore J, Rasmussen RK, Ajose-Adeogun AO, Nakayama T, Graham JA, Demur C, Hercend T, Diu-Hercend A, et al. VX-680, a potent and selective small-molecule inhibitor of the Aurora kinases, suppresses tumor growth in vivo. Nat Med 2004; 10:262-7; PMID:14981513; http://dx.doi.org/10.1038/nm1003
17. Hirota T, Lipp JJ, Toh BH, Peters JM. Histone H3 serine 10 phosphorylation by Aurora B causes HP1 dissociation from heterochromatin. Nature 2005; 438:1176-80; PMID:16222244; http://dx.doi.org/10.1038/nature04254
18. van Vugt MA, Brás A, Medema RH. Polo-like kinase-1 controls recovery from a G2 DNA damage-induced arrest in mammalian cells. Mol Cell 2004; 15:799-811; PMID:15350223; http://dx.doi.org/10.1016/j.molcel.2004.07.015
19. Bassermann F, Frescas D, Guardavaccaro D, Busino L, Peschiaroli A, Pagano M. The Cdc14B-Cdh1-Plk1 axis controls the G2 DNA-damage-response checkpoint. Cell 2008; 134:256-67; PMID:18662541; http://dx.doi.org/10.1016/j.cell.2008.05.043
20. Steegmaier M, Hoffmann M, Baum A, Lénárt P, Petronczki M, Krssák M, Gürtler U, Garin-Chesa P, Lieb S, Quant J, et al. BI 2536, a potent and selective inhibitor of polo-like kinase 1, inhibits tumor growth in vivo. Curr Biol 2007; 17:316-22; PMID:17291758; http://dx.doi.org/10.1016/j.cub.2006.12.037
21. Gascoigne KE, Taylor SS. Cancer cells display profound intra- and interline variation following prolonged exposure to antimitotic drugs. Cancer Cell 2008; 14:111-22; PMID:18656424; http://dx.doi.org/10.1016/j.ccr.2008.07.002
22. Zachos G, Black EJ, Walker M, Scott MT, Vagnarelli P, Earnshaw WC, Gillespie DAF. Chk1 is required for spindle checkpoint function. Dev Cell 2007; 12:247-60; PMID:17276342; http://dx.doi.org/10.1016/j.devcel.2007.01.003
23. Peddibhotla S, Lam MH, Gonzalez-Rimbau M, Rosen JM. The DNA-damage effector checkpoint kinase 1 is essential for chromosome segregation and cytokinesis. Proc Natl Acad Sci U S A 2009; 106:5159-64; PMID:19289837; http://dx.doi.org/10.1073/pnas.0806671106
24. Tang J, Erikson RL, Liu X. Checkpoint kinase 1 (Chk1) is required for mitotic progression through negative regulation of polo-like kinase 1 (Plk1). Proc Natl Acad Sci U S A 2006; 103:11964-9; PMID:16873548; http://dx.doi.org/10.1073/pnas.0604987103
25. Bayani J, Squire JA. Advances in the detection of chromosomal aberrations using spectral karyotyping. Clin Genet 2001; 59:65-73; PMID:11260203; http://dx.doi.org/10.1034/j.1399-0004.2001.590201.x
26. Karpenshif Y, Bernstein KA. From yeast to mammals: recent advances in genetic control of homologous recombination. DNA Repair (Amst) 2012; 11:781-8; PMID:22889934; http://dx.doi.org/10.1016/j.dnarep.2012.07.001
27. Blackwood E, Epler J, Yen I, Flagella M, O'Brien T, Evangelista M, Schmidt S, Xiao Y, Choi J, Kowanetz K, et al. Combination drug scheduling defines a "window of opportunity" for chemopotentiation of gemcitabine by an orally bioavailable, selective ChK1 inhibitor, GNE-900. Mol Cancer Ther 2013; 12:1968-80; PMID:23873850; http://dx.doi.org/10.1158/1535-7163.MCT-12-1218
28. Chen Z, Xiao Z, Gu WZ, Xue J, Bui MH, Kovar P, Li G, Wang G, Tao Z-F, Tong Y, et al. Selective Chk1 inhibitors differentially sensitize p53-deficient cancer cells to cancer therapeutics. Int J Cancer 2006; 119:2784-94; PMID:17019715; http://dx.doi.org/10.1002/ijc.22198
29. Ganzinelli M, Carrassa L, Crippa F, Tavecchio M, Broggini M, Damia G. Checkpoint Kinase 1 Down-Regulation by an Inducible Small Interfering RNA Expression System Sensitized In vivo Tumors to Treatment with 5-Fluorouracil 2008:5131-41
30. Bunz F, Dutriaux A, Lengauer C, Waldman T, Zhou S, Brown JP, Sedivy JM, Kinzler KW, Vogelstein B. Requirement for p53 and p21 to sustain G2 arrest after DNA damage. Science 1998; 282:1497-501; PMID:9822382; http://dx.doi.org/10.1126/science.282.5393.1497
31. Garner E, Raj K. Protective mechanisms of p53-p21-pRb proteins against DNA damage-induced cell death. Cell Cycle 2008; 7:277-82; PMID:18235223; http://dx.doi.org/10.4161/cc.7.3.5328
32. Parker LL, Piwnica-Worms H. Inactivation of the p34cdc2-cyclin B complex by the human WEE1 tyrosine kinase. Science 1992; 257:1955-7; PMID:1384126; http://dx.doi.org/10.1126/science.1384126
33. De Witt Hamer PC, Mir SE, Noske D, Van Noorden CJF, Würdinger T. WEE1 kinase targeting combined with DNA-damaging cancer therapy catalyzes mitotic catastrophe. Clin Cancer Res 2011; 17:4200-7; PMID:21562035; http://dx.doi.org/10.1158/1078-0432.CCR-10-2537
34. Maya-Mendoza A, Petermann E, Gillespie DAF, Caldecott KW, Jackson DA. Chk1 regulates the density of active replication origins during the vertebrate S phase. EMBO J 2007; 26:2719-31; PMID:17491592; http://dx.doi.org/10.1038/sj.emboj.7601714
35. Petermann E, Woodcock M, Helleday T. Chk1 promotes replication fork progression by controlling replication initiation. Proc Natl Acad Sci U S A 2010; 107:16090-5; PMID:20805465; http://dx.doi.org/10.1073/pnas.1005031107
36. Scorah J, McGowan CH. Claspin and Chk1 regulate replication fork stability by different mechanisms. Cell Cycle 2009; 8:1036-43; PMID:19270516; http://dx.doi.org/10.4161/cc.8.7.8040
37. Walton MI, Eve PD, Hayes A, Valenti M, De Haven Brandon A, Box G, Boxall KJ, Aherne GW, Eccles SA, Raynaud FI, et al. The preclinical pharmacology and therapeutic activity of the novel CHK1 inhibitor SAR-020106. Mol Cancer Ther 2010; 9:89-100; PMID:20053762; http://dx.doi.org/10.1158/1535-7163.MCT-09-0938
38. Young JD, Yao SYM, Sun L, Cass CE, Baldwin SA. Human equilibrative nucleoside transporter (ENT) family of nucleoside and nucleobase transporter proteins. Xenobiotica 2008; 38:995-1021; PMID:18668437; http://dx.doi.org/10.1080/00498250801927427
39. Carrassa L, Damia G. Unleashing Chk1 in cancer therapy. Cell Cycle 2011; 10:2121-8; PMID:21610326; http://dx.doi.org/10.4161/cc.10.13.16398
40. Matthews DJ, Yakes FM, Chen J, Tadano M, Bornheim L, Clary DO, Tai A, Wagner JM, Miller N, Kim YD, et al. Pharmacological abrogation of S-phase checkpoint enhances the anti-tumor activity of gemcitabine in vivo. Cell Cycle 2007; 6:104-10; PMID:17245119; http://dx.doi.org/10.4161/cc.6.1.3699
41. McNeely S, Conti C, Sheikh T, Patel H, Zabludoff S, Pommier Y, Schwartz G, Tse A. Chk1 inhibition after replicative stress activates a double strand break response mediated by ATM and DNA-dependent protein kinase. Cell Cycle 2010; 9:995-1004; PMID:20160494; http://dx.doi.org/10.4161/cc.9.5.10935
42. Syljuasen RG, Sorensen CS, Hansen LT, Fugger K, Lundin C, Johansson F, Helleday T, Sehested M, Lukas J, Bartek J. Inhibition of Human Chk1 Causes Increased Initiation of DNA Replication, Phosphorylation of ATR Targets, and DNA Breakage. 2005:3553-62
43. Parsels LA, Morgan MA, Tanska DM, Parsels JD, Palmer BD, Booth RJ, Denny WA, Canman CE, Kraker AJ, Lawrence TS, et al. Gemcitabine sensitization by checkpoint kinase 1 inhibition correlates with inhibition of a Rad51 DNA damage response in pancreatic cancer cells. Mol Cancer Ther 2009; 8:45-54; PMID:19139112; http://dx.doi.org/10.1158/1535-7163.MCT-08-0662
44. Costanzo V. Brca2, Rad51 and Mre11: performing balancing acts on replication forks. DNA Repair (Amst) 2011; 10:1060-5; PMID:21900052; http://dx.doi.org/10.1016/j.dnarep.2011.07.009
45. On KF, Chen Y, Ma HT, Chow JPH, Poon RYC. Determinants of mitotic catastrophe on abrogation of the G2 DNA damage checkpoint by UCN-01. Mol Cancer Ther 2011; 10:784-94; PMID:21430130; http://dx.doi.org/10.1158/1535-7163.MCT-10-0809
46. Riesterer O, Matsumoto F, Wang L, Pickett J, Molkentine D, Giri U, Milas L, Raju U. A novel Chk inhibitor, XL-844, increases human cancer cell radiosensitivity through promotion of mitotic catastrophe. Invest New Drugs 2011; 29:514-22; PMID:20024691; http://dx.doi.org/10.1007/s10637-009-9361-2
47. Andersen JL, Johnson CE, Freel CD, Parrish AB, Day JL, Buchakjian MR, Nutt LK, Thompson JW, Moseley MA, Kornbluth S. Restraint of apoptosis during mitosis through interdomain phosphorylation of caspase-2. EMBO J 2009; 28:3216-27; PMID:19730412; http://dx.doi.org/10.1038/emboj.2009.253
48. Mitchell JB, Choudhuri R, Fabre K, Sowers AL, Citrin D, Zabludoff SD, Cook JA. In vitro and in vivo radiation sensitization of human tumor cells by a novel checkpoint kinase inhibitor, AZD7762. Clin Cancer Res 2010; 16:2076-84; PMID:20233881; http://dx.doi.org/10.1158/1078-0432.CCR-09-3277
49. Origanti S, Cai SR, Munir AZ, White LS, Piwnica-Worms H. Synthetic lethality of Chk1 inhibition combined with p53 and/or p21 loss during a DNA damage response in normal and tumor cells. Oncogene 2013; 32:577-88; PMID:22430210; http://dx.doi.org/10.1038/onc.2012.84
50. Innocente SA, Lee JM. p53 is a NF-Y- and p21-independent, Sp1-dependent repressor of cyclin B1 transcription. FEBS Lett 2005; 579:1001-7; PMID:15710382; http://dx.doi.org/10.1016/j.febslet.2004.12.073
51. Xiao Z, Xue J, Gu W-Z, Bui M, Li G, Tao Z-F, Lin N-H, Sowin TJ, Zhang H. Cyclin B1 is an efficacy-predicting biomarker for Chk1 inhibitors. Biomarkers 2008; 13:579-96; PMID:18671143; http://dx.doi.org/10.1080/13547500802063240
52. Hirai H, Iwasawa Y, Okada M, Arai T, Nishibata T, Kobayashi M, Kimura T, Kaneko N, Ohtani J, Yamanaka K, et al. Small-molecule inhibition of Wee1 kinase by MK-1775 selectively sensitizes p53-deficient tumor cells to DNA-damaging agents. Mol Cancer Ther 2009; 8:2992-3000; PMID:19887545; http://dx.doi.org/10.1158/1535-7163.MCT-09-0463
53. Di Marco M, Di Cicilia R, Macchini M, Nobili E, Vecchiarelli S, Brandi G, Biasco G. Metastatic pancreatic cancer: is gemcitabine still the best standard treatment? (Review). [Review]. Oncol Rep 2010; 23:1183-92; PMID:20372829; http://dx.doi.org/10.3892/or_00000749
54. Borisy AA, Elliott PJ, Hurst NW, Lee MS, Lehar J, Price ER, Serbedzija G, Zimmermann GR, Foley MA, Stockwell BR, et al. Systematic discovery of multicomponent therapeutics. Proc Natl Acad Sci U S A 2003; 100:7977-82; PMID:12799470; http://dx.doi.org/10.1073/pnas.1337088100
55. Pandita A, Bayani J, Paderova J, Marrano P, Graham C, Barrett M, Prasad M, Zielenska M, Squire JA. Integrated cytogenetic and high-resolution array CGH analysis of genomic alterations associated with MYCN amplification. Cytogenet Genome Res 2011; 134:27-39; PMID:21508638; http://dx.doi.org/10.1159/000324698
56. Schröck E, du Manoir S, Veldman T, Schoell B, Wienberg J, Ferguson-Smith MA, Ning Y, Ledbetter DH, Bar-Am I, Soenksen D, et al. Multicolor spectral karyotyping of human chromosomes. Science 1996; 273:494-7; PMID:8662537; http://dx.doi.org/10.1126/science.273.5274.494